

## RESEARCH ARTICLE

### Preparation, Characterization and *in vitro* Anticancer Evaluation of Albendazole-Loaded Zinc Oxide Nanoparticles

Iqra Liaquat<sup>1\*</sup>, Muhammad Ovais Omer<sup>1\*</sup>, Muhammad Adil Rasheed<sup>1</sup> and Sohail Raza<sup>2</sup>

<sup>1</sup>Department of Pharmacology and Toxicology, University of Veterinary and Animal Sciences, Lahore, Pakistan;

<sup>2</sup>Institute of Microbiology, University of Veterinary and Animal Sciences Lahore, Pakistan 54000

\*Corresponding author: [drovaisomer@uvas.edu.pk](mailto:drovaisomer@uvas.edu.pk)

#### ARTICLE HISTORY (24-538)

Received: September 1, 2024  
Revised: November 6, 2024  
Accepted: November 14, 2024  
Published online: November 22, 2024

#### Key words:

Albendazole  
Anticancer activity  
Cancer  
Cell lines  
Nanoparticles  
Zinc oxide

#### ABSTRACT

Albendazole is a broad-spectrum anti-parasitic drug gaining attention for its promising anti-cancer activities in human and animal studies. Breast cancer is among the most prevalent and diverse malignancies affecting women. Conventional chemotherapy faces various limitations, such as development of multidrug resistance. Nanoparticles emerge as a promising alternative to overcome multidrug resistance in targeted cancer treatment. This study examined the anticancer effects of Albendazole combined with Zinc Oxide nanoparticles (ZnO NPs). The Albendazole-loaded Zinc Oxide nanoparticles (ALB ZnO NPs) were prepared and a 1:1 ratio was selected for further investigation because of the maximum percentage yield. Entrapment and loading efficacy were estimated at 80.3 and 40.2% respectively. Drug release in gastric media was significantly improved over time. Physicochemical characterization revealed maximum absorbance at 261nm, average size of 128nm with a zeta potential of +28.1mV, and smooth spherical morphology. FTIR spectra shift further confirmed the successful chemical bonding of Albendazole with ZnO NPs. MTT assay revealed ALB ZnO NPs induce dose dependent apoptosis in MCF-7 breast cancer cells. IC<sub>50</sub> of Albendazole was reduced from 84.85 µg/mL to 43.35 µg/mL when combined with ZnO NPs indicated marked increase in therapeutic potency. Furthermore, selective index of 4.057 reveals ALB ZnO NPs have high selective cytotoxicity towards cancer cells with a favorable safety profile for normal Vero cells. These findings suggest that ALB ZnO NPs have potential as targeted therapeutic strategy in breast cancer treatment, offering a more effective and selective alternative to conventional chemotherapy.

**To Cite This Article:** Liaquat I, Omer MO, Rasheed MA and Raza S, 2024. Preparation, characterization and *in vitro* anticancer evaluation of albendazole-loaded zinc oxide nanoparticles. Pak Vet J, 44(4): 1338-1344. <http://dx.doi.org/10.29261/pakvetj/2024.282>

#### INTRODUCTION

Mammary tumors are common in female dogs, resembling human breast cancer in many ways, and are a leading cause of death in both species. It is a significant concern in both human and veterinary medicine, with female dogs facing a higher lifetime risk of mammary tumors compared to women (Vazquez *et al.*, 2023). Every year, millions of women worldwide lose their lives due to breast cancer. It is one of the leading causes of death, accounting for 2.3 million cases globally each year, according to Global Cancer Observatory (GLOBOCAN) data (Tagde *et al.*, 2022). Chemotherapy, radiotherapy, surgery, and hormone therapy are currently used to treat cancer; however, there are several serious drawbacks,

including poor quality of life due to their side effects, inadequate drug concentration at tumor sites, lack of specificity, and untargeted drug delivery (Islam *et al.*, 2022).

Albendazole (ALB), methyl [5-(propylthio)-1H-benzimidazol-2-yl] carbamate, is a broad-spectrum anti-parasitic agent, first introduced in 1975 for treatment of liver flukes, tapeworms, lung and gastrointestinal nematodes in livestock (Theodorides *et al.*, 1976). It was subsequently approved for human use in 1982 (Dayan, 2003). Moreover, it has shown promise as anti-cancer drug. It blocks the targeted parasite's microtubule establishments (Capece *et al.*, 2009). Research reveals that ALB also shows significant anticancer properties by inhibiting glucose uptake, inducing oxidative stress,

promoting genetic material fragmentation, and activating apoptosis leading to cell death (Castro *et al.*, 2016; Sultana *et al.*, 2022). ALB is effective even against resistant cancer cells and it is approved for treatment as adjuvant in standard therapy (Son *et al.*, 2020; Lin *et al.*, 2020).

Cancer equally affects animals and rural communities, with resistance to treatments becoming a growing issue. Nanotechnology improves existing drugs by enhancing delivery, targeting, and reducing side effects (Sanabria, 2021). Nanoparticles based therapies have emerged as promising strategies for overcoming the limitations associated with conventional chemotherapy. They offer a range of potential benefits, including targeted delivery of drugs, increased bioavailability, and improved efficacy of chemotherapeutic agents (Zhang *et al.*, 2022).

Zinc Oxide nanoparticles (ZnO NPs) are important metal oxides because of their remarkable properties and utilization in multiple fields (Hassan *et al.*, 2024). Zinc oxide nanoparticles (ZnO NPs) have increasingly been recognized as an effective strategy for improving the solubility of poorly water-soluble drugs, such as albendazole (Qadeer *et al.*, 2022). ZnO NPs possess a high surface area relative to their volume, which enhances the interaction between the drug and the solvent, thereby promoting faster dissolution (Mudunkotuwa *et al.*, 2012). Additionally, their biocompatibility, low toxicity, and stability make them well-suited for pharmaceutical applications. The versatile physicochemical properties of ZnO NPs, including the potential for surface modifications, further support their ability to enhance solubility (Anjum *et al.*, 2021). Previous studies have demonstrated that ZnO NPs can significantly improve both the solubility and bioavailability of various hydrophobic drugs, providing a solid rationale for their application in enhancing the solubility of albendazole in this study (Nedra *et al.*, 2017). ZnO NPs have applications in displaying desirable biomedical purposes, such as antibacterial, drug delivery, diabetes treatment, anticancer, anti-inflammation, wound healing, and bioimaging (Kalpana *et al.*, 2018). Moreover, these particles are recognized as safe by the FDA (Jiang and Cai, 2018). ZnO NPs induce apoptosis by generating reactive oxygen species and increasing the oxidative stress on treated cells (Moungjaroen *et al.*, 2006). ZnO NPs induce powerful apoptosis in the breast cancer cells in a human cell line (MCF-7) and murine (TUBO cell line and cancer model) (Mahdizadeh *et al.*, 2019). An eclectic range of nanomaterials has been applied to veterinary practice, including diagnostic, pharmaceuticals, vaccines, and feed additives (Abdul Hannan *et al.*, 2024).

This study aimed to formulate nano formulation by entrapping Albendazole into Zinc Oxide nanoparticles and assess their *in vitro* anticancer effects. Specifically, the study aimed to compare the efficacy of Albendazole and Zinc Oxide nanoparticles alone, and the combination as Albendazole-loaded Zinc Oxide nanoparticles on MCF-7 (breast cancer) cell lines. Additionally, the induction of apoptosis for these formulations was evaluated and compared using the Vero cell line (healthy cells) and MCF-7 (breast cancer cell line).

## MATERIALS AND METHODS

**Chemicals:** Albendazole, zinc nitrate hexahydrate, sodium hydroxide, Tween 80, acetic acid (1% v/v), dialysis membrane, bovine serum, MTT dye, Dimethyl sulfoxide and Dulbecco's modified Eagle medium (DMEM).

**Preparation of albendazole zinc nanoparticles:** Zinc Oxide nanoparticles (ZnO NPs) were synthesized by precipitation in which 0.5 zinc nitrate solution (100 ml), was heated and added to 200ml NaOH solution, continued stirring for 3 hours at 70°C temperature. Suspension was calcined to obtain the dry powder of ZnO NPs. The amount of ZnO NPs was fixed in five different beakers and 0.15g, 0.3g, 0.45g, 0.6, and 0.75g of Albendazole was added to achieve 1:0.25, 1:0.5, 1:0.75, 1:1, 1:2.5 ZnO NPs to Albendazole ratio respectively. Tween 80 (1% v/v) was added dropwise. The resulting mixture was subjected to lyophilized (Alley *et al.*, 1988)

**Percentage yield:** Lyophilized powdered ALB ZnO NPs were used to determine the % yield. The powder was compared with the total amount of Albendazole and ZnO NPs used in the formulation (Akhlaq *et al.*, 2023).

$$\text{Percentage yield} = \frac{\text{weight of ALB ZnO NPs}}{\text{weight of (Albendazole + ZnO NPs)}} \times 100\%$$

**Evaluation of drug Entrapment and Loading in Nanoparticles:** The quantity of untrapped Albendazole in ALB ZnO NPs was assessed by utilizing a calibration curve (ranging from 300 to 7.5µg) (Racoviceanu *et al.*, 2020). The entrapment and loading efficiency were calculated by using the following equations (Anand *et al.*, 2021).

$$\text{Entrapment Efficacy} = \frac{\text{Amount of Albendazole Entrapped}}{\text{Total amount of Albendazole added}} \times 100\%$$

$$\text{Loading Efficacy} = \frac{\text{Amount of Albendazole Entrapped}}{\text{weight of Albendazole Zinc Oxide NPs}} \times 100\%$$

**Continuous *in vitro* drug release from ALB ZnO NPs:** *In vitro* dissolution investigations were performed by using spectrophotometer gastric and basic media (Manuja *et al.*, 2022).

### Physicochemical Characterization of Nanoparticles:

**UV Spectrophotometry:** The ultraviolet absorbance spectra of ALB ZnO NPs within the range of wavelength spanning from 200-1100nm were observed to confirm the successful loading of the drug into nanoparticles. (Anand *et al.*, 2021).

**Evaluation of Particle Size and Polydispersity Index /Zeta-Potential:** The dynamic light scattering technique, utilizing a Zetasizer (Malvern, U.K.), was employed to measure the size, zeta potential (ZP), and polydispersity index (PDI) of ALB ZnO NPs (Bayat *et al.*, 2021).

**Scanning Electron Microscopy (SEM):** The morphology of nanoparticles was measured by using a scanning electron microscope. The air-dried sample was analyzed by placing on a stub of SEM and secondary electron detector (Soltanzadeh *et al.*, 2021).

**Fourier Transform Infrared (FTIR):** This analysis utilized an attenuated total reflectance FTIR spectrometer with wavelength range 4000–400  $\text{cm}^{-1}$  (Selim *et al.*, 2020).

**Apoptosis assay (MTT):** Cell apoptosis was assessed utilizing the MTT assay. MCF-7 (breast cancer cells) and Vero (normal cells) obtained from UVAS Laboratory, were cultured in a 96-well microtiter plate and incubated in the  $\text{CO}_2$  incubator. Albendazole, ZnO NPs, and ALB ZnO NPs were consecutively diluted twofold in specific DMEM, resulting in treatment concentrations ranging from 1000 to 1.95  $\mu\text{g}$  per mL in individual groups. 100  $\mu\text{L}$  of each drug dilution was added and incubated for 24 hrs. Subsequently, 100  $\mu\text{L}$  MTT dye was added to each well and incubate for 3 hours. The optical density of each well was measured using an ELISA reader at 570 nm to calculate percentage inhibition (Al-otaibi, 2021).

$$\text{Percentage inhibition} = \left(1 - \frac{\text{ODt} - \text{ODb}}{\text{ODc} - \text{ODb}}\right) \times 100$$

In this context, ODt (test), ODc (control), and ODb (blank) denote the average optical densities.

**IC<sub>50</sub> and selectivity index:** The concentrations of treatments needed to induce apoptosis by 50% (IC<sub>50</sub>) were identified using CompuSyn software and selectivity index (S.I) was computed (Swanepoel *et al.*, 2019).

$$\text{S.I} = \frac{\text{IC}_{50} \text{ of drug in normal cell line}}{\text{IC}_{50} \text{ of drug in cancer cell line}}$$

## RESULTS

**Percentage yield of ALB ZnO NPs and estimation of entrapment and loading efficiency:** The percentage yield of Albendazole with different ZnO NPs concentrations was measured. The yield percentages were determined as follows: 80.12% ( $\pm 0.075$ ), 58.66% ( $\pm 0.069$ ), 69.25% ( $\pm 0.042$ ), 63.17% ( $\pm 0.042$ ), 83.33% ( $\pm 0.032$ ), and 60.43% ( $\pm 0.061$ ) for the ratios 1:0, 1:0.25, 1:0.50, 1:0.75, 1:1, and 1:1.25, respectively. Among these, the ratio of 1:1 was chosen for further study because of its highest yield i.e. 83.33% ( $\pm 0.032$ ). ALB ZnO NPs suspension was centrifuged and the supernatant was retained containing non-entrapped Albendazole in a nanocarrier. A standard calibration curve of Albendazole (250, 125, 62.5, 31.2, 15.6 & 7.8  $\mu\text{g}$ ) was constructed to measure unknown concentrations of drug in ALB ZnO NPs. The entrapment and loading efficiency were found 80.3 and 40.2% respectively.

**Continuous *in vitro* drug release from ALB ZnO NPs:** The Albendazole concentration released from the ALB ZnO NPs, was calculated based on calibration lines. The

analysis of Albendazole release from ALB ZnO NPs (Fig. 1) revealed a Bi-phasic pattern. Initially, there was a burst observed which later followed by the sustained release of drug. This modified release pattern confirms the effective capture of Albendazole within ALB ZnO NPs.

## Characterization of Nanoparticles

**UV-Spectrophotometry, ZETA sizer and SEM:** The successful entrapment of Albendazole in ZnO NPs was confirmed through UV-visible spectrophotometry between 200 and 400 nm with a peak at 261 nm as shown in Fig. 2(A). The PDI of 0.217 and the diameter of 128 nm for ALB ZnO NPs, respectively, demonstrate the stable formulation of these particles in Fig. 2(B). Zeta potential predicts stability of nanoparticles in suspension as its high absolute values (positive or negative) indicate higher electrostatic repulsion, thereby ensuring the stability of the formulation. In the case of ALB ZnO NPs, a zeta potential of +28.1 mV indicates sufficient repulsive forces to stabilize the particles, promoting effective dispersion and minimizing aggregation Fig. 2(C). Scanning electron microscopy (SEM) of ALB ZnO NPs illustrate round and spherical, with smooth surface morphology Fig. 2(D).

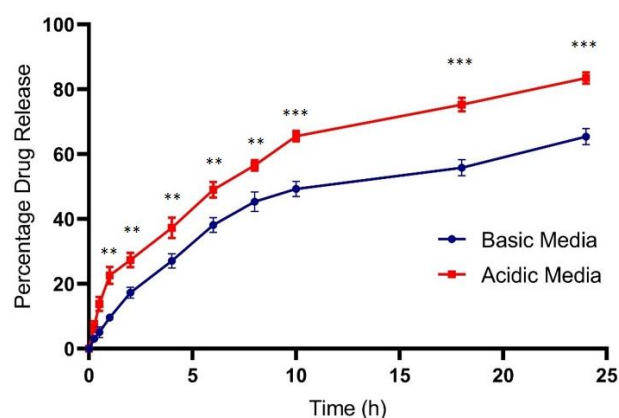


**Fig. 1:** *In vitro* dissolution profiles of ALB ZnO NPs show significantly ( $P=0.002$ ) improved percentage release of drug in gastric media as compared to basic media. Significant differences between drug release (mean and S.D) in acidic and basic media are indicated by asterisks (\*  $P < 0.05$ , \*\*  $P < 0.01$ , \*\*\*  $P < 0.001$ ).

**Fourier Transform infrared spectroscopy (FTIR):** Fig. 3 displays the FTIR spectra of Albendazole, ZnO NPs, and ALB ZnO NPs. The following classifications were given to the primary different peaks found in the Albendazole spectrum: N-H carbamate stretching ( $3323.3 \text{ cm}^{-1}$ ); C-H aliphatic stretching vibration ( $2956.8 \text{ cm}^{-1}$ ); amide stretching imidazole ( $1710.85$  and  $1265.30 \text{ cm}^{-1}$ ); C=O bond bending vibration in carbamate ( $1150.5 \text{ cm}^{-1}$ ); N-H bending out of plane in benzimidazole class ( $694.37 \text{ cm}^{-1}$ ). The primary typical bands found in the spectrum of ZnO NPs were identified as follows: the band associated with the fingerprint region, whose peak at  $1440$  and  $975.6 \text{ cm}^{-1}$  corresponds to C-N and C-O stretch, respectively; the C-H stretch of alkane at a peak at approximately  $2956.78 \text{ cm}^{-1}$ . The existence of a peak at  $829.39$ ,  $1384.5$ ,  $1710.7$ , and  $2175.7 \text{ cm}^{-1}$  in the ALB ZnO NPs IR spectra is indicative of the peak shift of Albendazole due to bonding with ZnO NPs.

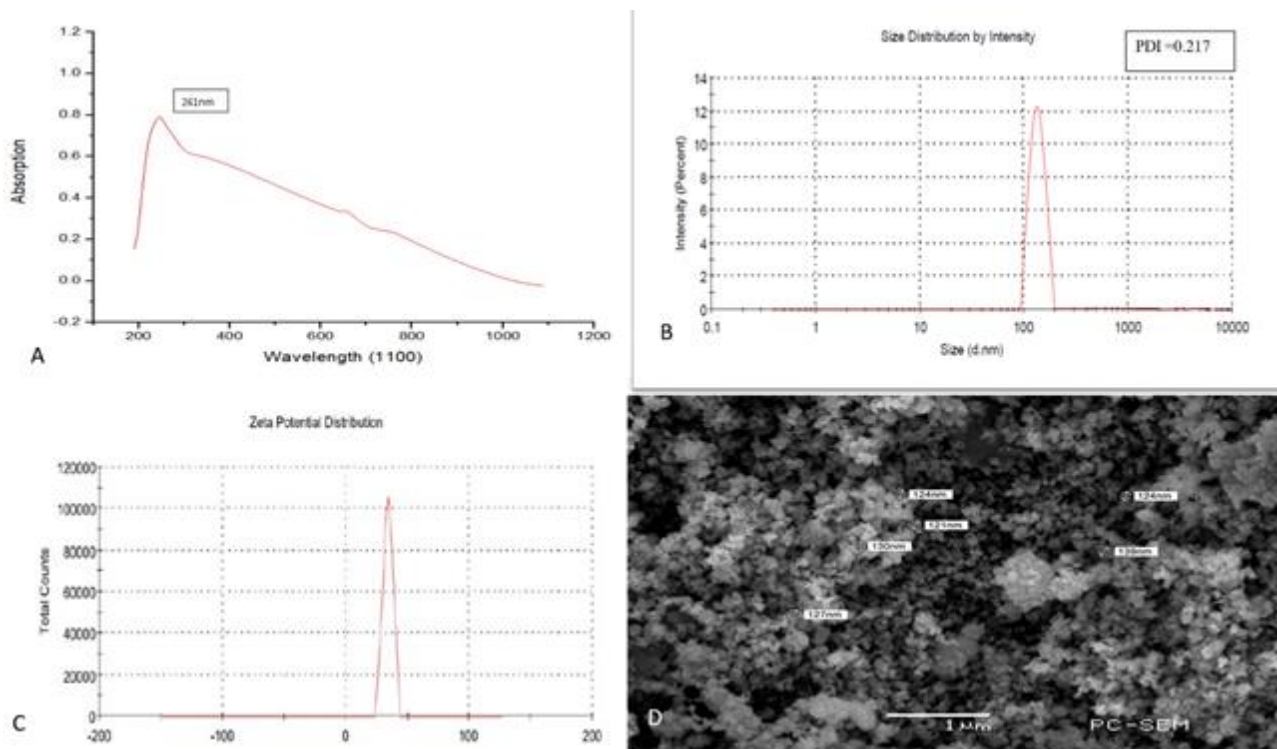


**Fig. 2: (A)** The absorption spectra of ALB ZnO NPs with the highest peak of 261 nm indicate Albendazole presence. **(B)** Zeta size 128 nm and **(C)** zeta potential of +28.1 mV charge. **(D)** SEM of ALB ZnO NPs with spherical and smooth surfaces.

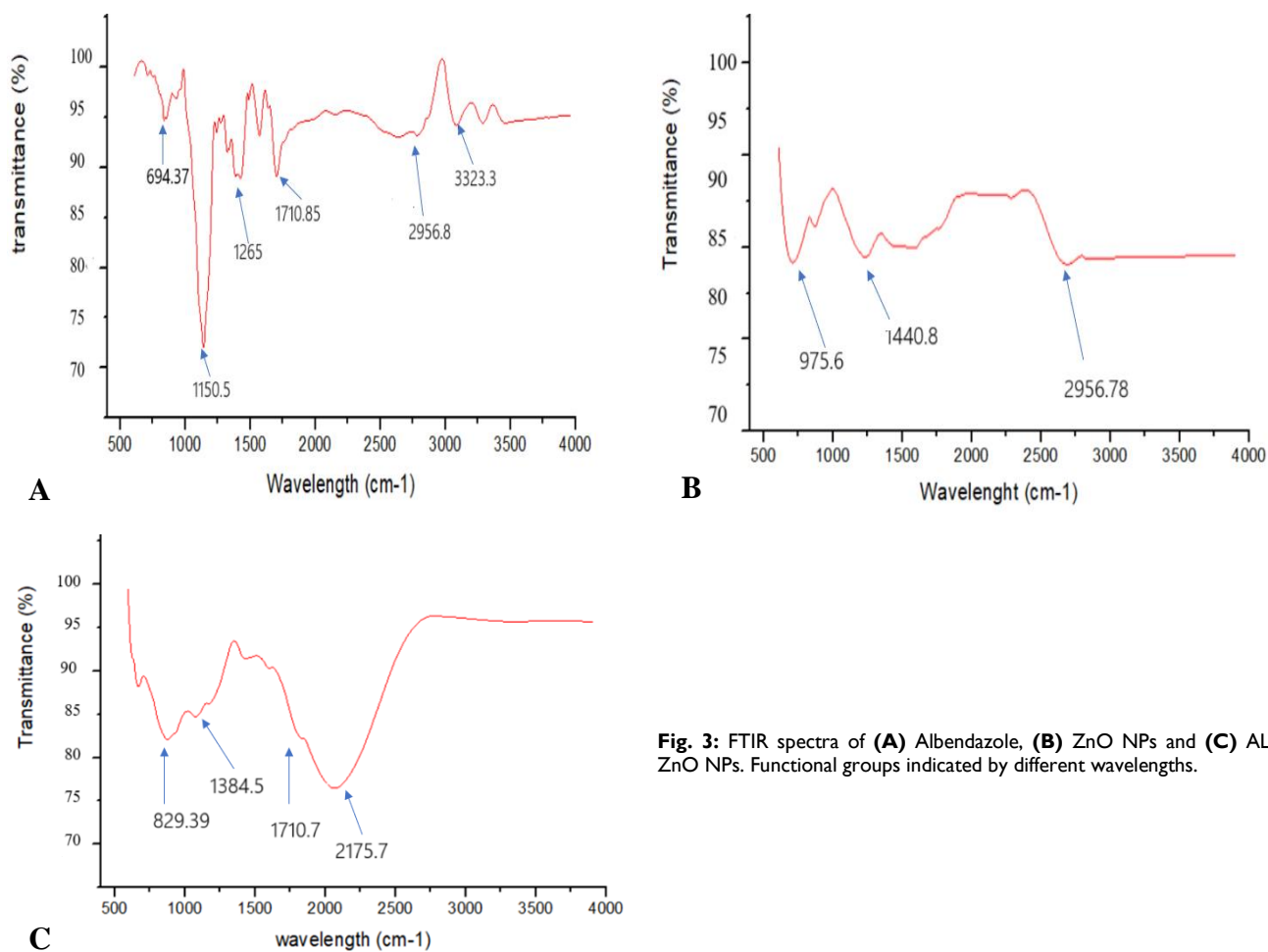


**Fig. 3: FTIR spectra of (A) Albendazole, (B) ZnO NPs and (C) ALB ZnO NPs. Functional groups indicated by different wavelengths.**

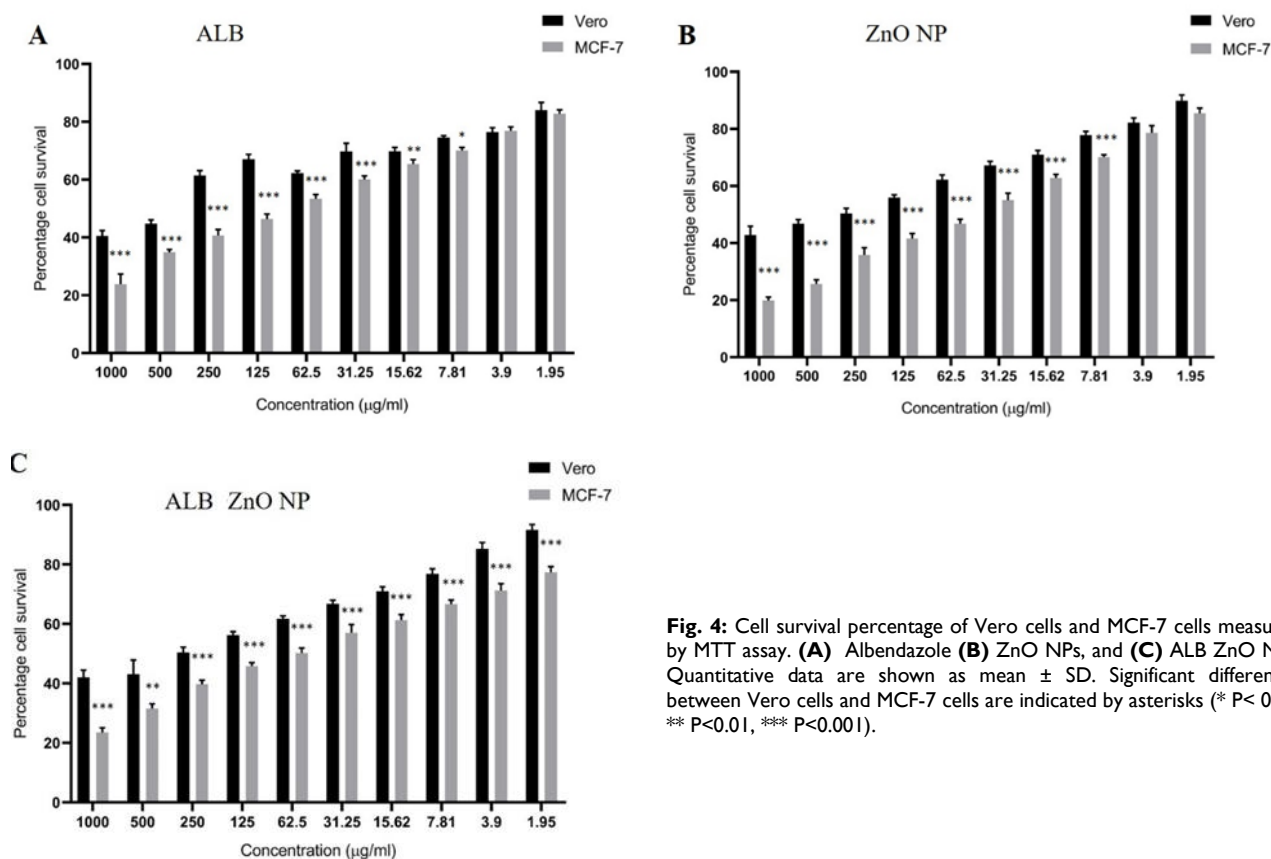


**Fig. 4:** Cell survival percentage of Vero cells and MCF-7 cells measured by MTT assay. **(A)** Albendazole **(B)** ZnO NPs, and **(C)** ALB ZnO NPs. Quantitative data are shown as mean  $\pm$  SD. Significant differences between Vero cells and MCF-7 cells are indicated by asterisks (\*  $P < 0.05$ , \*\*  $P < 0.01$ , \*\*\*  $P < 0.001$ ).

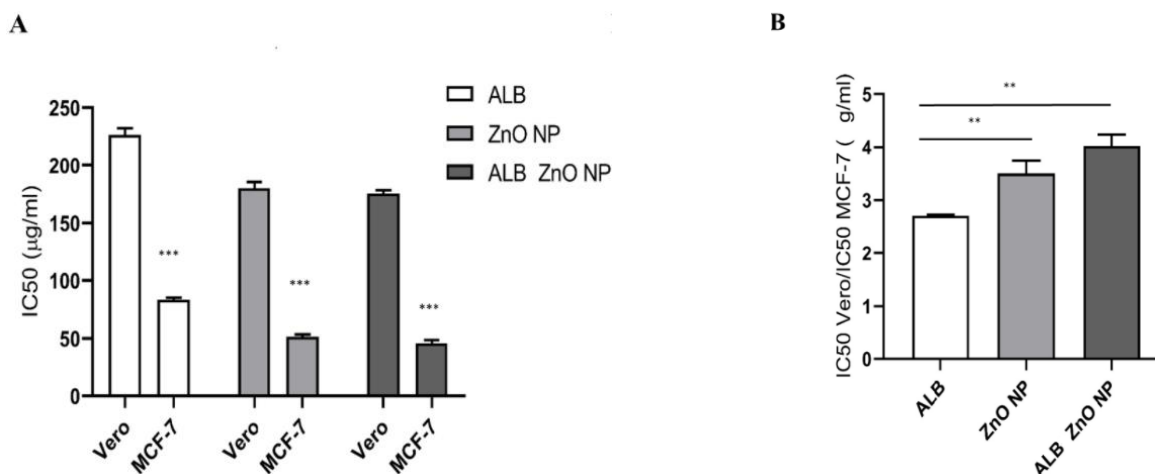


**Fig. 5:** **(A)** IC50 values (µg/ml) of Vero cells and MCF-7 cells **(B)** Selectivity index is significantly increase for the ZnO NP group and ALB ZnO NPs as compare to albendazole alone. Quantitative data are shown as mean  $\pm$  SD. Significant differences between treatments are indicated by asterisks (\*  $P < 0.05$ , \*\*  $P < 0.01$ , \*\*\*  $P < 0.001$ ).

**Anticancer Activity:** Anticancer activity by MTT assay was performed on cancerous cell lines (MCF-7) and non-cancerous cell lines (Vero). The inhibition of MCF-7 and Vero cell growth and induction of apoptosis was assessed using a range of single drug concentrations (1000–1.95 µg/mL) by measuring mitochondrial activity through the MTT assay. The IC50 values, representing the concentration needed to reduce cell viability by 50%, were calculated with CompuSyn software. The study found that the drugs induced apoptosis more on the MCF-7 cell line, compared to the Vero cell line (Fig. 4). However, none of the drugs alone were cytotoxic to Vero cells. Selectivity Index (SI) values, derived from the IC50

(µg/mL) of the individual drugs on Vero cells relative to MCF-7 cells, are shown in Fig. 5B. An SI greater than 3 indicates significant anticancer potential and selective toxicity towards cancer cells. The IC50 values for Albendazole, ZnO NPs, and ALB ZnO NPs on MCF-7 cells were 84.85, 50.93, and 43.35 µg/mL, respectively. For Vero cells, the IC50 values were 232.1, 183.55, and 175.88 µg/mL, respectively. The combination of ZnO NPs with Albendazole notably reduced the IC50 on MCF-7 cells compared to single-drug treatments. Overall, drug combinations showed greater cytotoxicity to MCF-7 cells, as evidenced by lower IC50 values, compared to individual drug treatments (Fig. 5).

## DISCUSSION

Cancer develops through complicated cellular changes, notably involving disrupted microtubule function that affects chromosome segregation. In breast cancer, such microtubule disruptions contribute to uncontrolled cell growth, making them significant targets for therapeutic intervention (Siegel *et al.*, 2024). Chemotherapy remains a prevalent treatment approach for cancer, however its effectiveness is hindered by inadequate target specificity and emergence of drug resistance (Wang *et al.*, 2023). Recently, Albendazole has been found to have anti-tumor activities in preclinical studies and a small number of clinical inquiries have been reported (Chai *et al.*, 2021). Albendazole exhibits anticancer effects by blocking glycolysis (Abolhassani *et al.*, 2012) and an increase in reactive oxygen species synthesis in cancer cells (Nygren *et al.*, 2013). Albendazole is a hydrophobic drug and its clinical application is limited because of its less solubility (Patel *et al.*, 2011; Tanaka *et al.*, 2013). Nano formulation of Albendazole has been synthesized to improve the hydrophilicity and biological availability of the drug (Movahedi *et al.*, 2017). Zinc Oxide nanoparticles (ZnO NPs) are gaining attention because of their high biocompatibility (Raguvaran *et al.*, 2015) and synergistic anticancer activity (Wiesmann *et al.*, 2020).

In this study, ZnO NPs were prepared by co-precipitation method and Albendazole was adsorbed on its surface. The supreme percentage yield of Albendazole-loaded Zinc Oxide nanoparticles (ALB ZnO NPs) was calculated with a concentration of ZnO NPs to ALB of 1:1, and this ratio was selected for further investigation. This result verified a previous report in which Albendazole copper oxide nanoparticles were formulated with the same ratio (Zafar *et al.*, 2016). Entrapment and loading efficiencies are the criteria typically used to assess the ability of nanoparticles to retain drug and were found to be 80% and 40% respectively for ALB ZnO NPs. These results correlate with azithromycin Zinc Oxide nanoparticle studies which have almost similar efficacies (Saddik *et al.*, 2022). *In vitro* release of Albendazole from ALB ZnO NPs was rapid in the first phase due to surface absorption of drug, and later entrapped drug was released better in a gastric medium compared to the basic medium. Similar release pattern was also observed in another nano formulation of Albendazole polyurethane nanoparticles (Racoviceanu *et al.*, 2020) (Rao *et al.*, 2024).

Absorption of UV spectra for ALB ZnO NPs was observed at 261nm which is supported by UV spectral analysis of Albendazole combination with zinc nanoparticles, studied for antiparasitic action (Shakibaie *et al.*, 2022). Zeta potential and size of ALB ZnO NPs described the 28.1mV positive charge and 128nm size, respectively. It has been demonstrated in previous studies that a positive charge of particles affects cell survival (Prach *et al.*, 2013; Omidi *et al.*, 2024). SEM analysis matches with Albendazole solid polymer nanoparticles showed notable morphological modifications after drug loading (Racoviceanu *et al.*, 2020). The FTIR spectra of ZnO NPs exhibited characteristic peaks that aligned with study of Hamdy *et al.* (2023). FTIR spectra indicated no additional functional groups or bonds, confirming

Albendazole remained intact without significant chemical interaction (Zafar *et al.*, 2016).

The anticancer effect of Albendazole is justified through various cellular actions, apoptosis, (Fatima *et al.*, 2024), decreased angiogenesis, (Gaikwad *et al.*, 2023) and block glucose uptake (Son *et al.*, 2020; Dik *et al.*, 2021). Albendazole-loaded polyurethane nanoparticles demonstrated anticancer activity by inducing apoptosis (Racoviceanu *et al.*, 2020). Meanwhile Guruviah *et al.* (2020) investigated ZnO NPs decreased cell viability of cancer cell lines. Our study provided an insight into the enhanced anticancer potential of Albendazole through loading in ZnO NPs against MCF-7 cancer cells. The increased anticancer effect may originate from synergistic interaction between Albendazole and ZnO nanoparticles. In the present study, a dose-dependent reduction in cell count was observed, and IC50 values of Albendazole and ZnO nanoparticles decreased when used in combination. The selective index shows ALB ZnO NPs have more selective potent cytotoxic effect on breast cancer MCF-7 cell line. This synergistic effect arises from dual mechanism of action, Albendazole inhibiting tubulin polymerization leads to disruption of microtubules which impaired cell division, while Zinc Oxide nanoparticles induce production of ROS triggering apoptosis through oxidative stress.

In conclusion, ALB ZnO NPs exhibit significant anticancer potential, but additional preclinical and clinical research is essential to assess their efficacy, safety, and applicability in clinical settings. These studies are critical for validation of this novel nanocarrier system as practical therapeutic option in clinical setting.

**Authors contribution:** Iqra Liaquat: investigation, writing- original draft preparation and methodology. Muhammad Ovais Omer: supervision, conceptualization, and reviewing. Final approval for the submission. Muhammad Adil Rasheed: data curation and visualization. Sohail Raza: software validation and data analysis.

## REFERENCES

- Abdul H, Xiaoxia Du, Bakhtawar M, *et al.*, 2024. Nanoparticles as potent allies in combating antibiotic resistance: A promising frontier in antimicrobial therapy. *Pak Vet J* DOI:10.29261/pakvetj/2024.227
- Abolhassani M, Guais A, Sanders E, *et al.*, 2012. Screening of well-established drugs targeting cancer metabolism: reproducibility of the efficacy of a highly effective drug combination in mice. *Invest New Drug* 30:1331-1342.
- Akhlaq A, Ashraf M, Omer MO, *et al.*, 2023. Carvacrol-fabricated chitosan nanoparticle synergistic potential with topoisomerase inhibitors on breast and cervical cancer cells. *ACS omega*. 8(35):31826-31838.
- Al-otaibi, W. 2021. Rosemary oil nano-emulsion potentiates the apoptotic effect of mitomycin C on cancer cells *in vitro*. *Pharmacia* 68:201-209.
- Alley M, Scudiero D, Monks A, *et al.*, 1988. Feasibility of drug screening with panels of human tumor cell lines using a microculture tetrazolium assay. *Cancer Res* 48(3):589-601.
- Anand T, Anbukkarasi M, Thomas PA, *et al.*, 2021. A comparison between plain eugenol and eugenol-loaded chitosan nanoparticles for prevention of *in vitro* selenite-induced cataractogenesis. *J Drug Deliv Sci tec.* 65:102696.
- Anjum S, Hashim M, Malik SA, *et al.*, 2021. Recent advances in zinc oxide nanoparticles (ZnO NPs) for cancer diagnosis, target drug delivery, and treatment. *Cancers* 13(18):4570.

- Bayat S, Zabihi AR, Farzad SA, et al., 2021. Evaluation of debridement effects of bromelain-loaded sodium alginate nanoparticles incorporated into chitosan hydrogel in animal models. *Iran J Basic Med Sci* 24(10):1404.
- Capece, Bettencourt PS, Guillermo LV, et al., 2009. Enantiomeric behaviour of albendazole and fenbendazole sulfoxides in domestic animals: pharmacological implications. *Vet J* 181(3):241-250.
- Castro L, Kwiecinski, M, Ourique F, et al., 2016. Albendazole as a promising molecule for tumor control. *Redox Biol* 10:90-99.
- Chai JY, Jung BK and Hong SJ, 2021. Albendazole and mebendazole as anti-parasitic and anti-cancer agents: an update. *Korean J Parasit* 59(3):189.
- Dayan AD, 2003. Albendazole, mebendazole and praziquantel. Review of non-clinical toxicity and pharmacokinetics. *Acta Trop* 86:141-159.
- Dik B, Coşkun D, and Bahçivan E, et al., 2021. Potential antidiabetic activity of benzimidazole derivative albendazole and lansoprazole drugs in different doses in experimental type 2 diabetic rats. *Turkish J Med Sci* 51(3):1579-1586.
- Fadwa AO, Alkoblan DK, Mateen A, et al., 2021. Synergistic effects of zinc oxide nanoparticles and various antibiotics combination against *Pseudomonas aeruginosa* clinically isolated bacterial strains. *Saudi J Biol Sci* 28(1):928-935.
- Fatima I, Ahmad R, Barman S, et al., 2024. Albendazole inhibits colon cancer progression and therapy resistance by targeting ubiquitin ligase RNF20. *Brit J Cancer* 130(6):1046-1058.
- Guruviah K, Annamalai SK, Ramaswamy A, et al., 2020. Comparative antimicrobial and anticancer activity of biologically and chemically synthesized zinc oxide nanoparticles toward breast cancer cells. *Nanomater* 10(4):272-283.
- Hamdy DA, Ismail MA, El-Askary H. M, et al., 2023. Newly fabricated zinc oxide nanoparticles loaded materials for therapeutic nano delivery in experimental cryptosporidiosis. *Sci Rep-Uk* 13(1):19650.
- Hassan MH, Emam IA, Farghali H, et al., 2024. Toxicological screening of zinc oxide nanoparticles in mongrel dogs after seven days of repeated subcutaneous injections. *BMC Vet Res* 20(1):476.
- Islam MR, Islam F, Nafady MH, et al., 2022. Natural small molecules in breast cancer treatment: understandings from a therapeutic viewpoint. *Molecules* 27(7):2165.
- Jiang J, Pi J and Cai J. 2018. The advancing of zinc oxide nanoparticles for biomedical applications. *Bioinorg Chem Appl* 1062562.
- Kalpna V and Devi RV. 2018. A review on green synthesis, biomedical applications, and toxicity studies of ZnO NPs. *Bioinorg Chem Appl* 3569758.
- Lin Y, Ong YC, Keller S, et al., 2020. Synthesis, characterization and antiparasitic activity of organometallic derivatives of the anthelmintic drug albendazole. *Dalton Transactions* 49(20):6616-6626.
- Mahdizadeh R, Homayouni M, Neamati A, et al., 2019. Green synthesized-zinc oxide nanoparticles, the strong apoptosis inducer as an exclusive antitumor agent in murine breast tumor model and human breast cancer cell lines (MCF7). *J Cell Biochem* 120(10):17984-17993.
- Manuja A, Kumar B, Athira S, et al., 2022. Zinc oxide nanoparticles encapsulated in polysaccharides alginate/gum acacia and iron oxide nanomaterials show enhanced biocompatibility and permeability to intestinal barrier. *Food Hydrocoll* 11th 2-100050.
- Moungjaroen J, Nimmannit U, Callery PS, et al., 2006. Reactive oxygen species mediate caspase activation and apoptosis induced by lipoic acid in human lung epithelial cancer cells through Bcl-2 down-regulation. *J Pharmacol Exp Ther* 319(3):1062-1069.
- Movahedi F, Li L, Gu W, et al., 2017. Nanoformulations of albendazole as effective anticancer and antiparasite agents. *Nanomedicine* 12(20):2555-2574.
- Mudunkotuwa IA, Rupasinghe T, Wu CM, et al., 2012. Dissolution of ZnO nanoparticles at circumneutral pH: a study of size effects in the presence and absence of citric acid. *Langmuir* 28(1):396-403.
- Nedra K, Ariyaratna I, Welideniya D, et al., 2017. Nanotechnological strategies to improve water solubility of commercially available drugs. *Curr Nano* 7(2):84-110.
- Nygren P, Fryknäs M, Ågerup B, et al., 2013. Repositioning of the anthelmintic drug mebendazole for the treatment of colon cancer. *J Cancer Res & Clin Oncol* 139:2133-2140.
- Patel K, Doudican NA, Schiff PB, et al., 2011. Albendazole sensitizes cancer cells to ionizing radiation. *Radiat Oncol* 6:1-7.
- Prach M, Stone V and Proudfoot L, 2013. Zinc oxide nanoparticles and monocytes: Impact of size, charge and solubility on activation status. *Toxicol Appl Pharm* 266(1):19-26.
- Qadeer A, Ullah H, Sohail M, et al., 2022. Potential application of nanotechnology in the treatment, diagnosis, and prevention of schistosomiasis. *Front Bioeng Biotech* 10:1013354.
- Omidi F, Hajarian H, Karamishabankareh H, et al., 2024. Comparison of the Effect of Adding Different Levels of Zinc Chloride, Curcumin, Zinc Oxide Nanoparticles (Zano-NPs), Curcumin Loaded on Zano-NPs on Post-Thawing Quality of Ram Semen. *Vet Med Sci* 10(6):e70091.
- Racoviceanu R, Trandafirescu C, Voicu M, et al., 2020. Solid polymeric nanoparticles of albendazole: synthesis, physico-chemical characterization and biological activity. *Molecules* 25(21):5130.
- Rao MRP and Sakharwade SA, 2024. Enhancement of Solubility of Albendazole by Inclusion Complexation with Nanosponges and  $\beta$ -Cyclodextrin. *Indian J Pharm Educ* 58(1):S306-S315.
- Raguvaran R, Manuja A, and Manuja BK, 2015. Zinc oxide nanoparticles: opportunities and challenges in veterinary sciences. *Immun. Res.* 11(2), 1.
- Saddik MS, Elsayed MM, El-Mokhtar MA, et al., 2022. Tailoring of novel azithromycin-loaded zinc oxide nanoparticles for wound healing. *Pharmaceutics* 14(1):111.
- Sanabria R, 2021. Nanotechnological improvement of veterinary anthelmintics. *Pharma Nano* 9(1):5-14.
- Siegel RL, Giaquinto AN and Jemal A, 2024. Cancer statistics, 2024. *Cancer J Clin* 74(1).
- Selim YA, Azb MA, Ragab I, et al., 2020. Green synthesis of zinc oxide nanoparticles using aqueous extract of *Deverra tortuosa* and their cytotoxic activities. *Sci Report* 10(1):3445.
- Shakibaie M, Khalaf AK, Rashidipour M, et al., 2022. Effects of green synthesized zinc nanoparticles alone and along with albendazole against hydatid cyst protoscolices. *Ann Med Surg* 78.
- Soltanzadeh M, Peighambari SH, Ghanbarzadeh B, et al., 2021. Chitosan nanoparticles as a promising nanomaterial for encapsulation of pomegranate (*Punica granatum*) peel extract as a natural source of antioxidants. *Nanomaterials* 11(6):1439.
- Son DS, Lee ES and Adunyah SE, 2020. The antitumor potentials of benzimidazole anthelmintics as repurposing drugs. *Immune Netw* 20(4).
- Sultana T, Jan U, and Lee, JI, 2022. Double repositioning: Veterinary antiparasitic to human anticancer. *Int J Mol Sci* 23(8), 4315.
- Swanepoel B, Nitulescu G M, Olaru O T et al., 2019. Anti-cancer activity of a 5-aminopyrazole derivative lead compound (BC-7) and potential synergistic cytotoxicity with cisplatin against human cervical cancer cells. *Int J Mol Sci* 20(22):5559.
- Tagde P, Najda A, Nagpal K, et al., 2022. Nanomedicine-based delivery strategies for breast cancer treatment and management. *Int J Mol Sci* 23(5):2856.
- Tanaka Y, Waki R and Nagata S, 2013. Species differences in the dissolution and absorption of griseofulvin and albendazole, biopharmaceutics classification system class II drugs, in the gastrointestinal tract. *Drug Metabol Pharmacol* 28(6), 485-490.
- Theodorides VJ, Gyurik RJ, Kingsbury WD, et al., 1976. Anthelmintic activity of albendazole against liver flukes, tapeworms, lung and intestinal roundworms. *Experientia* 32:702-703.
- Vazquez E, Lipovka Y, Cervantes-Arias A, et al., 2023. Canine mammary cancer: State of the art and future perspectives. *Animals* 13(19):3147.
- Wang C, Wang Q, Wang H, et al., 2023. Hydroxyethyl starch-folic acid conjugates stabilized theranostic nanoparticles for cancer therapy. *J Control Rel* 353:391-410.
- Wiesmann N, Tremel W and Brieger J, 2020. Zinc oxide nanoparticles for therapeutic purposes in cancer medicine. *J Material Chem B* 8(23):4973-4989.
- Zafar A, Ahmad I, Ahmad A, et al., 2016. Copper (II) oxide nanoparticles augment antifilarial activity of Albendazole: *In vitro* synergistic apoptotic impact against filarial parasite *Setaria cervi*. *Int J Pharma* 501(1-2):49-64.
- Zhang C, Zhou X, Zhang H, et al., 2022. Recent progress of novel nanotechnology challenging the multidrug resistance of cancer. *Front Pharmacol* 13:776895.